THE JOURNAL OF BIOLOGICAL CHEMISTRY VOL. 288, NO. 7, pp. 4557–4566, February 15, 2013

Superoxide Triggers an Acid Burst in *Saccharomyces cerevisiae* to Condition the Environment of Glucose-starved Cells*

Received for publication, August 13, 2012, and in revised form, December 20, 2012 Published, JBC Papers in Press, December 31, 2012, DOI 10.1074/jbc.M112.409508

J. Allen Baron[1], **Kaitlin M. Laws, Janice S. Chen, and Valeria C. Culotta**[2]

From the Department of Biochemistry and Molecular Biology, Johns Hopkins University Bloomberg School of Public Health, Baltimore, Maryland 21205

Background: During prolonged periods without glucose yeast cells acidify the extracellular environment.
Results: This acid burst is derived from a mitochondrial aldehyde dehydrogenase and a cascade involving superoxide damage to the TCA cycle.
Conclusion: The acid burst can condition the medium to improve cell growth.
Significance: Damage from mitochondrial superoxide can be advantageous to cells during carbon starvation stress.

Although yeast cells grown in abundant glucose tend to acidify their extracellular environment, they raise the pH of the environment when starved for glucose or when grown strictly with non-fermentable carbon sources. Following prolonged periods in this alkaline phase, *Saccharomyces cerevisiae* cells will switch to producing acid. The mechanisms and rationale for this "acid burst" were unknown. Herein we provide strong evidence for the role of mitochondrial superoxide in initiating the acid burst. Yeast mutants lacking the mitochondrial matrix superoxide dismutase (SOD2) enzyme, but not the cytosolic Cu,Zn-SOD1 enzyme, exhibited marked acceleration in production of acid on non-fermentable carbon sources. Acid production is also dramatically enhanced by the superoxide-producing agent, paraquat. Conversely, the acid burst is eliminated by boosting cellular levels of Mn-antioxidant mimics of SOD. We demonstrate that the acid burst is dependent on the mitochondrial aldehyde dehydrogenase Ald4p. Our data are consistent with a model in which mitochondrial superoxide damage to Fe-S enzymes in the tricarboxylic acid (TCA) cycle leads to acetate buildup by Ald4p. The resultant expulsion of acetate into the extracellular environment can provide a new carbon source to glucose-starved cells and enhance growth of yeast. By triggering production of organic acids, mitochondrial superoxide has the potential to promote cell population growth under nutrient depravation stress.

Cells exist and thrive in environments that are both supportive of life and potentially hostile. The environment is in a constant state of change and the onset of stress conditions, such as nutrient depravation and exposure to toxins, require appropriate adaptation strategies. Cells have evolved a variety of mechanisms to appropriately sense and respond to variations in the environment through induction of stress pathways and adjustments in metabolism. Yet, in some cases, cells respond by modifying the microenvironment itself to enhance its suitability for their fitness and survival. The pathogen *Plasmodium falciparum*, for example, is known to secrete a variety of proteins that enhance the permeability of the red blood cell membrane to increase the availability of nutrients (1). Cancer cells are particularly adept at altering microenvironments. During the process of invasion, these cells secrete a variety of metalloproteases (2) and also acidify their surrounding environment to inhibit the toxic activity of immune cells and chemotherapies, and promote migration to more nutrient-rich environments (3, 4). To make nutrients more accessible, the bakers' yeast *Saccharomyces cerevisiae* secretes phospholipases (5), a variety of enzymes that break down sugars (6), and phosphatases (7).

To *S. cerevisiae*, the pH of the environment is critical for regulating growth and survival (8–10). Cells growing on the preferred carbon source glucose acidify the surrounding media by activating the proton ATPase, Pma1p (11), and secreting organic acids (12, 13). This acidic environment (≈pH 4–5) helps to maintain the electrochemical gradient across the plasma membrane and drive uptake of many essential nutrients (14). On the other hand, when yeast cells grow on the less preferred non-fermentable carbon sources or are starved for glucose, they alkalize their surrounding environment, which slows growth but enhances survival under stress (8, 15, 16). This period of alkalization correlates with increases in volatile ammonia that serves as a signaling molecule to synchronize colony growth (15–18). Interestingly, following prolonged growth on the non-fermentable carbon source glycerol, yeast cells can switch from this alkalization phase to producing acid (17, 19, 20). The mechanism or rationale for this sudden "acid burst" has been unknown. In previous studies completed by Palkova's group (17, 19, 20), the production of ammonia during the alkalization phase was reportedly defective in *S. cerevisiae* cells lacking the mitochondrial matrix manganese-containing superoxide dismutase, SOD2 (or yeast Sod2p). Sod2p was suggested to affect ammonia signaling, but through an unknown pathway (19, 21).

* This work was supported, in whole or in part, by National Institutes of Health Grants ES 08996 and GM 50016 (to V. C. C.) and the Johns Hopkins University NIEHS, National Institutes of Health, center.
[1] Supported by National Institutes of Health NCI Training Grant T32 CA009110.
[2] To whom correspondence should be addressed. Tel.: 410-955-3029; Fax: 410-955-2926; E-mail: vculotta@jhsph.edu.

Superoxide dismutases (SODs)[3] represent a family of metalloenzymes responsible for detoxifying superoxide radicals generated as a by-product of aerobic metabolism. Most eukaryotes, including *S. cerevisiae*, contain both a Mn-SOD2 in the mitochondrial matrix as well as, a Cu,Zn-containing SOD1 that is largely cytosolic but also found in the mitochondrial intermembrane space (22, 23). The presence of SODs on both sides of the mitochondrial inner membrane collectively protect against superoxide generated by the electron transport chain. The importance of SOD2 in guarding against mitochondrial oxidative damage has been underscored in various model organisms for SOD2 deficiency. *SOD2*−/*SOD2*− mice are neonatal lethal and early death in this case is thought to arise from severe oxidative damage to the mitochondrial respiratory chain (24, 25). Loss of SOD2 also induces early mortality in *Drosophila* adults, associated with damage to the mitochondrial respiratory chain and TCA (tricarboxylic acid) cycle enzymes (26). In the bakers' yeast *S. cerevisiae*, cells lacking Sod2p are viable but are highly sensitive to hyperoxia and redox cycling agents (27–29), defects ascribed to increased superoxide damage to mitochondrial components. However, the means by which loss of yeast mitochondrial matrix Sod2p can control extracellular pH as described earlier (19) is not clear, particularly because the superoxide substrate for Sod2p should not cross the mitochondrial membranes (30).

Here, we describe a new connection between mitochondrial superoxide and the control of environmental pH. Specifically we find that the acid burst produced by cells during long-term respiratory conditions can be induced by mitochondrial superoxide. With either mutation in yeast *SOD2* or by treatment with the redox cycler paraquat, the acid burst is accelerated in yeast cells starved for glucose. Moreover, the acid burst is eliminated through Mn-antioxidants that act as SOD mimics and remove intracellular superoxide. We provide evidence that superoxide damage to Fe-S enzymes in the TCA cycle results in massive production of acetate involving the mitochondrial aldehyde dehydrogenase Ald4p. The concomitant acetate burst during nutrient starvation provides a new carbon source to enhance cell growth during long-term nutrient depravation.

EXPERIMENTAL PROCEDURES

Yeast Strains—The yeast strains in this study were all derived from the parent strain BY4741 (*MAT*a, *his3*Δ*1, leu2*Δ*0, LYS2, met15*Δ*0, ura3*Δ*0*). Strains with single gene deletions were obtained from the *MAT*a haploid deletion library (Open Biosystems) and verified by sequencing in earlier studies (27) or in the current studies: *sod2*Δ, *sod1*Δ, *sdh2*Δ, *sdh4*Δ, *cyt1*Δ, *cox7*Δ, *cit1*Δ, *idh1*Δ, *kgd1*Δ, *lsc1*Δ, *fum1*Δ, *mdh1*Δ, *ald2*Δ, *ald3*Δ, *ald4*Δ, *ald5*Δ, *ald6*Δ, *pmr1*Δ. Strains LJ111 (*aco1*::*LEU2*) (gift of L. Jensen), CO217 (*coq1*::*LEU2*) (31), and LJ109 (*rho*$^-$) (32) were described previously. Strains JAB075 (*ald4*::*kanMX*, *sod2*::*URA3*) and AR148 (*pmr1*::*kanMX*, *sod2*::*URA3*; gift of A. Reddi) were created by transformation of the aforementioned *ald4*Δ and *pmr1*Δ strains, respectively, with the *sod2*Δ::*URA3* plasmid, pGSOD2 as described (33). Strain JAB069 (*ald4*::*kanMX*, *sdh4*::*HIS3*) was created by transformation of *ald4*Δ with a PCR-based *sdh4*::*HIS3* deletion cassette generated by amplifying *HIS3* from pRS403 (34) using as primers: forward primer, 5′-ACGCTTTCGACTTTCTTCCTACGCGCTTTATAATAGCTATGGCGGCATCAGAGCAGATTG-3′; reverse primer, 5′-GTTACATGACCGAACAAATGATTCGTGGTGATTTATCTACGTTTACAATTTCCTGATGCG-3′. Transformations were performed by the standard lithium acetate procedure (35).

Culture Conditions and pH Measurements—To examine the effects of yeast colony growth on extracellular pH, solid growth medium containing 3% glycerol (or where indicated, 2% glucose), 1% yeast extract, 0.01% bromocresol purple (BCP; Sigma, B5880), and 2% bacto-agar was prepared precisely as described by Palkova and co-workers (15), except supplemental $CaCl_2$ was generally omitted. pH was typically adjusted to 5.75 with HCl prior to autoclaving but could range from 4.35 (enhance detection of media alkalization) to 6.5 (enhance detection of media acidification) without altering the cell alkaline and acid phases. When needed, the specified concentrations of paraquat (MP Biomedicals) or $MnCl_2$ were added immediately before pouring. In all cases, extracellular pH was monitored using "giant colony" growth as prescribed by Palkova *et al.* (15) where 2×10^5 cells in 10 μl were spotted onto plates and incubated at 30 °C. Images were taken with a Sony Cybershot DSC-F828 on the days indicated. Cell viability measurements were obtained by removing cells at the designated times and measuring colony-forming units on YPD (1% yeast extract, 2% peptone, 2% glucose) averaged over 3 giant colonies as described (20). Results were normalized to WT at day 4. WT and *sod2*Δ strains retain full viability through day 8 and at day 11 exhibited 92 (S.D. ± 8) and 89% (S.D. ± 11) viability, respectively.

For monitoring effects of yeast growth under low glucose conditions, cells were inoculated at an initial $A_{600} = 0.05$ and grown shaking at 220 rpm, at 30 °C for 24 h in a liquid media consisting of 1% yeast extract and 0.2% glucose, adjusted to pH 5.5 with HCl. To determine the extracellular pH of these cultures, a colorimetric assay based on the pH-sensitive dyes BCP and bromocresol green (BCG; Sigma, 114359) was developed. Briefly, cells were removed by centrifugation at 17,000 × *g* for 1 min and the media was collected (90 μl each) in triplicate and applied to a 96-well plate. Water (blank), 0.1% BCP, or 0.1% BCG (10 μl) were added and absorbance was measured at A_{430}, A_{589}, A_{514}, and A_{616} in a Synergy HT Multi-Mode Microplate Reader (BioTek). pH was calculated by subtracting the absorbance of the blank at each wavelength and using the following empirically derived equations.

For BCP (pH ≥ 5.3),

$$\mathrm{pH} = 5.852 + 1.081 \times \mathrm{LOG}\left(\frac{A_{589}}{A_{430}}\right) \qquad \text{(Eq. 1)}$$

For BCG (pH < 5.3),

$$\mathrm{pH} = 4.590 - \mathrm{LOG}\left(\frac{5.963}{\left(\frac{A_{616}}{A_{514}}\right) - 0.045} - 1\right) \qquad \text{(Eq. 2)}$$

Plates were imaged on an HP Scanjet 8200 scanner. For conditioned media tests, cultures from low glucose conditions as

[3] The abbreviations used are: SOD, superoxide dismutase; TCA, tricarboxylic acid; BCP, bromocresol purple; PQ, paraquat; BCG, bromocresol green; SDH, succinate dehydrogenase.

described earlier were filter-sterilized (Millipore, Millex-GV, 0.22 μm) to remove cells and the conditioned medium collected was then used for inoculation of WT cells at $A_{600} = 0.1$ followed by aerobic growth for the indicated time points.

Metabolite Measurements—To measure glucose, acetate, and succinate concentrations in media, conditioned medium was collected from cells grown in low glucose as described earlier and cells were removed by centrifugation. Measurements were performed with a Synergy HT Multi-Mode Microplate Reader using the QuantiChrom™ Glucose Assay Kit (BioAssay Systems), the Acetic Acid kit (R-Biopharm), and the Succinic Acid kit (R-Biopharm), respectively, according to the manufacturers' specifications. To adapt the Acetic Acid and Succinic Acid kits to a plate reader format, one-tenth the recommended volumes were used and each reading was path length corrected using the standard correction of the plate reader: $(A_{977} - A_{900})/0.18$.

Intracellular acetate measurements were performed in the same manner as those for media, except cells were first lysed by glass bead homogenization in 20 mM potassium phosphate, 1.2 M sorbitol, 1.0 mM PMSF, pH 7.4, and clarified by centrifugation at 17,000 × *g* for 10 min. After determining the total protein by Bradford assay, lysates were heated 15 min at 85 °C and the supernatant was collected for analysis after a second centrifugation. Intracellular acetate concentrations were normalized to total protein.

To measure intracellular metabolites of the TCA cycle, cells grown as described earlier in low glucose media were harvested at $A_{600} = 1–1.2$ and washed in PBS. Cells were resuspended in PBS at a ratio of 5 μl of PBS/A_{600} cells and lysed by glass bead homogenization as described (36). Lysates were clarified by centrifugation at 17,000 × *g* for 10 min and total protein was determined by Bradford assay. Duplicate samples were analyzed by stable-isotope dilution GC-MS by the Kennedy Krieger Institute Biochemical Genetics Laboratory.

Enzymatic Assays—For measurements of aconitase and succinate dehydrogenase (SDH) activity, cells were collected from low glucose liquid media (10 ml) after 24 h growth by centrifugation or scraped from glycerol plates containing BCP (2–9 × 10^8 cells collected from strains plated as in Fig. 1*A*) on the days indicated and stored at −20 °C. Cells were then resuspended in lysis buffer consisting of 20 mM potassium phosphate, 1.2 M sorbitol, 1.0 mM PMSF, 0.1% Triton X-100, pH 7.4, at a ratio of 10 μl of buffer/2 × 10^7 cells and lysed by glass bead homogenization. Protein concentrations were determined by Bradford assay and enzymatic assay measurements were performed with 10–50 μg of lysate protein per reaction. Aconitase activity was measured as described (36) in 250 μl of total reaction volume and calculated as the nanomoles of *cis*-aconitate consumed per mg of protein per min using the Beer-Lambert law and an extinction coefficient of 4.88 mM^{-1} cm^{-1}. SDH activity was measured with the procedure of Ackrell *et al.* (37), adapted to a 200-μl 96-well plate format. Briefly, SDH in whole cell lysates was activated at 30 °C for 10 min in the reaction mixture without electron acceptors/dyes (178 μl volume; final concentration after addition of dyes = 20 mM potassium phosphate, 20 mM succinate or malonate, 1 mM KCN, pH 7.4). After 10 min, prewarmed dyes (22 μl volume; final concentration in complete reaction mix = 1 mM phenazine methosulfate (Sigma), 0.05 mM 2,6-dichlorindophenol (Sigma)) were added to initiate the reaction. SDH activity was calculated as the malonate-sensitive nanomoles of 2,6-dichlorindophenol reduced per mg of protein per minute using an extinction coefficient of 21 mM^{-1} cm^{-1}.

For Pma1p ATPase activity, cells were grown in 1% yeast extract with 2 or 0.2% glucose, pH 5.5 to an $A_{600} = 0.75–0.9$. Plasma membranes were isolated (38) and Pma1p ATPase activity was measured by assaying orthovanadate-sensitive release of inorganic phosphate precisely as described by Monk *et al.* (39) and normalized to the activity of WT cells grown in 0.2% glucose.

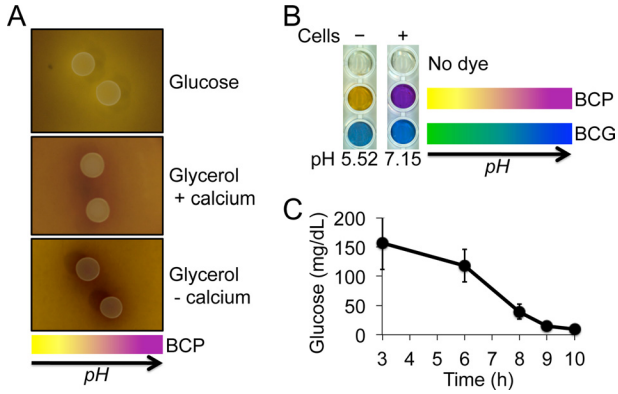

FIGURE 1. **Yeast cells alkalize their environment under respiratory conditions.** *A*, giant colonies (15) of WT BY4741 yeast cells were obtained by spotting 2 × 10^5 cells onto the indicated growth medium containing the pH indicator BCP and as carbon source either 2% glucose or 3% glycerol. Where indicated, medium was supplemented with 30 mM $CaCl_2$. Cells were photographed on the second day of growth. *B* and *C*, WT yeast cells were inoculated at $A_{600} = 0.05$ in a liquid media containing 0.2% glucose and following specific time points, cells were removed and extracellular medium analyzed for either glucose or pH. *B*, media pH was determined following 24 h of growth using BCP and BCG indicator dyes. Shown is a photograph of the media color change with the pH indicators and the corresponding pH value calculated as outlined under "Experimental Procedures." Numerical results represent the averages of triplicate analyses where S.D. ≤0.03. *Cells* − = growth media alone. *C*, extracellular glucose was determined at the indicated time points as described under "Experimental Procedures." Results represent the average of triplicate samples where *error bars* denote S.D. Illustrated in *A bottom* and *B right* are the gradient of color changes with BCP and BCG as pH ranges from acidic (BCP, *yellow*; BCG, *green*) to basic (BCP, *purple*; BCG, *blue*).

RESULTS

A Role for Superoxide and SOD2 in Controlling the Acid Burst of Respiring Cells—Extracellular pH in yeast growth medium is readily monitored by pH indicators such as BCP and BCG. When grown in high glucose, fermenting yeast cells rapidly acidify the medium (Fig. 1*A* top), but when grown on non-fermentable carbon sources, the respiring yeast cells initially elevate the extracellular pH (Fig. 1*A*, *middle* and *bottom*). As prescribed by Čáp *et al.* (19), this alkalization is observed on glycerol medium supplemented with 30 mM calcium (Fig. 1*A*, *middle*), yet is also seen without added calcium (Fig. 1*A*, *bottom*); hence all subsequent studies were conducted in the absence of calcium supplements. Alkalization of the growth medium is not unique to non-fermentable carbon sources, but is also observed in liquid cultures with low glucose, conditions where cells switch from fermentation to respiration (8) (Fig. 1*B*). Cells grown in 0.2% glucose rapidly deplete their glucose (Fig. 1*C*) and the pH of the extracellular medium rises from 5.5 to ≥7.0 within 24 h (Fig. 1*B*).

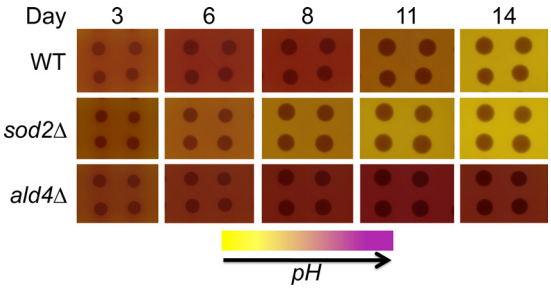

FIGURE 2. **Acid production following the alkaline phase of yeast cell growth is accelerated by *sod2*Δ mutations and eliminated by *ald4*Δ mutations.** The indicated yeast strains were analyzed for acid and base production following the designated times of incubation on glycerol containing plates (no calcium) as described in the legend to Fig. 1*A*.

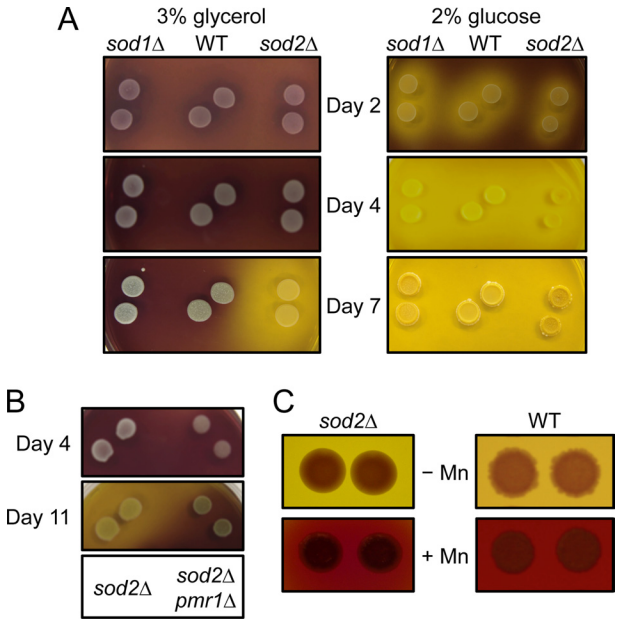

FIGURE 3. **Role of mitochondrial SOD2 and Mn-antioxidants in preventing the acid burst of respiratory cells.** Giant colonies of the indicated strains were plated under either respiratory, 3% glycerol (*A*, *left*, and *B* and *C*), or fermenting, 2% glucose (*A*, *right*), conditions as described in the legend to Fig. 1*A* and photographed on the designated days of incubation (*A* and *B*) or on days 11 (*sod2*Δ) or 16 (WT) (*C*). *C*, where indicated, plates were supplemented with 0.5 mM $MnCl_2$, a concentration that is non-toxic but sufficient to maximize intracellular levels of Mn-antioxidants that remove superoxide (44–50).

Following long-term growth on glycerol containing medium, *S. cerevisiae* cells can enter an acid phase as previously described, which we refer to herein as the acid burst (Fig. 2) (17, 19, 20). We observe that the initiation of the acid burst is substantially accelerated in strains lacking Mn-SOD2, the mitochondrial matrix manganese-containing SOD. The *sod2*Δ null cells show no defect in the initial alkalization of the medium (Fig. 2, Fig. 3*A*); however, their onset of entry into the acid phase is accelerated compared with WT strains (Fig. 2). This *sod2*Δ impact on extracellular pH appears specific to respiratory conditions, as *sod2*Δ cells are indistinguishable from WT cells in acid production under fermentative conditions with high glucose (Fig. 3*A*, *right*). Moreover, the early acid phase of *sod2*Δ cells under respiratory conditions is not due to accelerated death of these cells, because our viability tests (see "Experimental Procedures") estimate that WT and *sod2*Δ both retain ≈90% viability after 11 days on glycerol.

The premature acid burst appears specific to *sod2*Δ strains and was not observed in other yeast mutants we tested that control oxidative stress resistance. For example, deletion of genes required for glutathione and thioredoxin reduction in the mitochondria (*GLR1* (27) and *TRR2* (40)) did not show the same accelerated acid burst of *sod2*Δ cells, nor did deletion of the thioredoxin and glutathione peroxidases *AHP1* (41), *TSA1* (42), and *GPX1* (43) (data not shown). We also observed that loss of *SOD1*, encoding the cytosolic and mitochondrial intermembrane space Cu,Zn-SOD, does not induce a premature acid burst (Fig. 3*A*). The effects on extracellular pH appear specific to loss of SOD activity on the matrix side of the mitochondrial inner membrane.

In addition to SOD enzymes, yeast cells have the capacity to remove superoxide through the action of small non-proteinaceous complexes of manganese such as Mn-phosphate. These redox active compounds of manganese, so called Mn-antioxidants, are effective SOD mimics *in vitro* and in yeast cells *in vivo* (44–50). Mn-antioxidants are elevated when yeast cells accumulate high manganese through either supplementation of manganese salts to the growth medium or by mutations in the *pmr1*Δ Golgi pump for manganese (46–48). We observed that in both cases, the Mn-antioxidants prevented the premature acid burst of *sod2*Δ strains (Fig. 3, *B* and *C left*). Moreover, boosting levels of Mn-antioxidants in WT cells completely prevented cells from exiting the alkaline phase and the acid burst was eliminated (Fig. 3*C*, *right*). These studies together with results from *sod2*Δ cells strongly indicate that the transition to acid phase following long-term respiratory conditions is triggered by superoxide.

Redox cycling agents such as paraquat can induce production of cellular superoxide, including mitochondrial matrix superoxide (51–53). As seen in Fig. 4*A*, paraquat treatment dramatically accelerated the transition to the acid burst in glycerol and within 24 h, both WT and *sod2*Δ cells treated with paraquat were producing copious levels of acid. Much less paraquat was required in the case of *sod2*Δ cells (Fig. 4*A*), consistent with the anticipated high superoxide in these mutants that cannot catalytically remove mitochondrial matrix superoxide. In addition to effects on glycerol plates, paraquat treatment also caused cells grown in low glucose to produce acid rather than base (Fig. 4*B*). The paraquat-induced burst of acid was not due to cell death; in fact total cell growth over 24 h was slowed by only 25–30% with doses of paraquat that induced maximal acidification (Fig. 4*C*), which translates to an overall reduction in growth rate of only ≈15%. These studies support the notion that acid production during respiratory conditions can be induced by superoxide, specifically the mitochondrial superoxide relevant to Sod2p.

Fe-S Cluster Enzymes of the TCA Cycle as Targets of Superoxide during the Acid Burst—Superoxide can disrupt Fe-S clusters (54, 55), and we tested whether the mitochondrial Fe-S proteins SDH and aconitase were inhibited in cells producing acid. In WT cells, both aconitase and SDH are affected by paraquat. Aconitase is inhibited even by low (50 μM) levels of paraquat when cells are not producing acid, but maximal levels of SDH inhibition requires very high (800 μM) paraquat, conditions where WT cells produce acid (Fig. 5*A*). In *sod2*Δ cells, aconitase

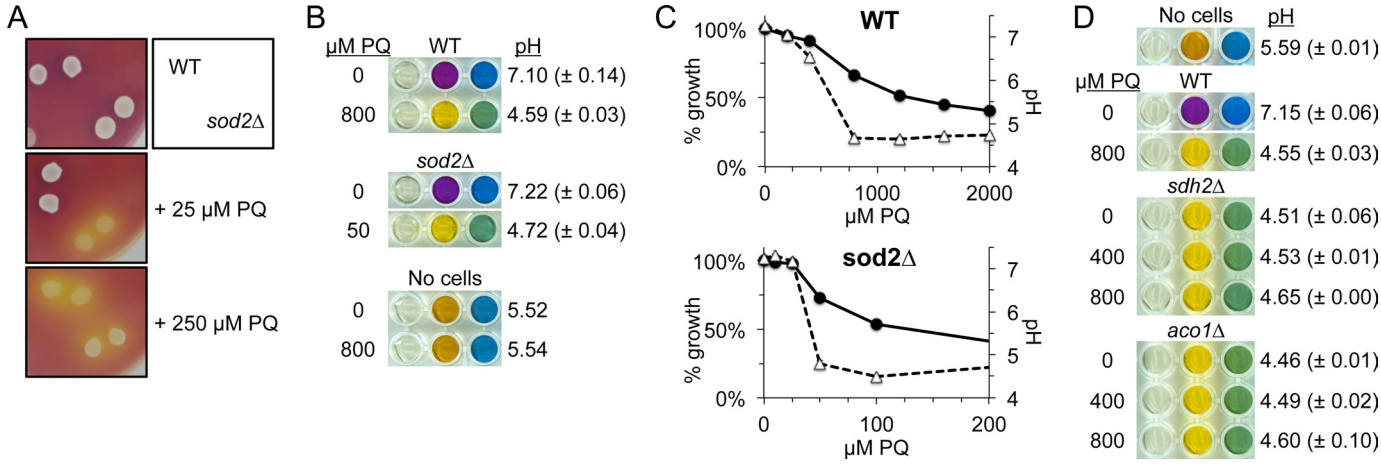

FIGURE 4. **Paraquat, as well as, mutations in aconitase or SDH lead to an acid burst under respiratory conditions.** The indicated yeast strains were grown either on glycerol containing medium for 2 days (*A*), or in low glucose liquid medium for 24 h (*B–D*) as described in the legend to Fig. 1. Where indicated, the growth medium was supplemented with the designated concentrations of paraquat (*PQ*). *B* and *C*, *open triangles,* and *D*, pH was calculated in triplicate as described in the legend to Fig. 1*B* where values in parentheses (*B* and *D*) denote S.D. *C*, cell growth (*black circles*) was measured turbidimetrically at A_{600} and plotted as a function of control cell growth with no paraquat.

is constitutively low without paraquat consistent with previous studies (55, 56), and the main effect of 50 μM paraquat is inhibition of SDH activity (Fig. 5*A*). Hence with WT and *sod2*Δ cells, acid production is associated with losses in both aconitase and SDH. The same trends were apparent with cells grown for extended periods on glycerol without paraquat: WT cells exhibited reductions in both aconitase and SDH, whereas *sod2*Δ cells are constitutively low in aconitase and lose SDH activity over time (Fig. 5*B*).

We tested whether the degree of SDH and aconitase inhibition observed *in vitro* reflected disruptions in the TCA cycle, *in vivo*. TCA cycle metabolites were measured from cells grown in low glucose and treated with paraquat. As controls, mutants of SDH and aconitase were used. Yeast *sdh4*Δ mutants have high succinate but low citrate, whereas *aco1*Δ mutants lacking aconitase have high citrate and low succinate (Fig. 5*C*). WT cells treated with 800 μM paraquat exhibited the elevation in succinate typical of *sdh* mutants, but did not lose citrate (Fig. 5*C*), consistent with the double inhibition of SDH and aconitase (as in Fig. 5*A*). In *sod2*Δ null cells treated with 50 μM paraquat, citrate was elevated consistent with losses in aconitase, but there was no loss of succinate (Fig. 5*C*), again consistent with TCA blockages in both SDH and aconitase.

The correlation between the acid burst and TCA cycle inhibition prompted us to test whether mutations in TCA cycle genes were by themselves able to induce an acid burst. As seen in Fig. 4*D*, the *aco1*Δ and *sdh2*Δ mutants lacking aconitase and SDH showed acid production in low glucose, analogous to what was seen with paraquat treatment. Moreover, there was no additive effect of paraquat, indicating that paraquat and loss of the TCA cycle operate in the same pathway to induce acid. Acid production is not specific to disruptions at aconitase and SDH, as mutations in citrate synthase (*cit1*Δ), α-ketoglutarate dehydrogenase (*kgd1*Δ), and fumarase (*fum1*Δ) all resulted in acid production (Table 1). Disruptions in 5 of 8 steps in the TCA cycle mimicked the effects of paraquat and induced acid production in low glucose. Only deletions in isocitrate dehydrogenase (*idh1*Δ), succinyl-CoA ligase (*lsc1*Δ), and malate dehydrogenase (*mdh1*Δ) resulted in little to no acid production (Table 1).

Because the TCA cycle is required for electron transport chain functioning, we addressed whether blockages in the electron transport chain also lead to the acid burst. As seen in Table 1, mutations that inhibit the electron transport chain, other than SDH loss, including deletions affecting ubiquinone, complex III, or complex IV, and *rho*$^-$ mutations lacking mitochondrial DNA, did not rapidly acidify the medium. Thus, it is not a general defect in mitochondrial function that leads to acid production in low glucose, but specific disruptions in the TCA cycle.

The Acid Burst Results from Acetate Production by the Aldehyde Dehydrogenase Ald4p—What is the source of the acid burst with low glucose? In the case of high glucose, yeast acidification of the environment involves activation of a cell surface proton ATPase Pma1p, as well as cellular export of organic acids (11–13). As seen in Fig. 6*A*, cells grown in low glucose have extremely low levels of Pma1p activity compared with cells grown in high glucose. However, Pma1p activity remained low in the TCA cycle mutants that produce acid (Fig. 6, *B* and *C*). We therefore examined effects of organic acids. Previous studies have shown that Fe-S cluster assembly or delivery defects result in extracellular acidification, marked by secretion of various organic acid mixtures (57–59) and, in yeast, *sdh3* and *sdh4* mutants secrete succinate (60). However, *sdh* mutants grown under glucose starvation conditions exhibit only small increases in extracellular succinate (Fig. 6*D*). The same is true with WT cells treated with paraquat (Fig. 6*D*). These small increases in extracellular succinate are not likely to account for the large changes in extracellular pH, and other acid producing cells (*e.g. cit1*Δ, *aco1*Δ, *kdg1*Δ, and *fum1*Δ) do not elevate extracellular succinate (Fig. 6*D*). Another organic acid more highly elevated in *sdh* mutants is acetate (61), which feeds into the TCA cycle via acetyl-CoA. WT yeast cells grown in high glucose produce abundant acetate (13) but with glucose-starved WT cells, extracellular acetate is virtually undetectable (Fig. 7*A*). Remarkably, when glucose-starved WT cells are treated with

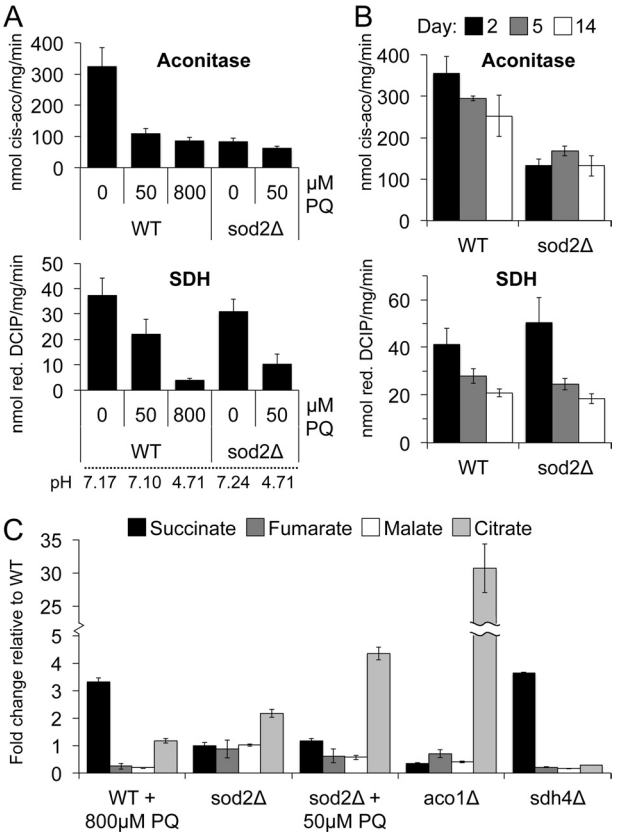

FIGURE 5. **Activities of aconitase and SDH under respiratory conditions.** *A* and *C*, the designated yeast strains were grown as described under "Experimental Procedures" in 0.2% glucose medium that was supplemented with the indicated concentrations of paraquat. *A*, extracellular pH shown at the *bottom* was measured in triplicate samples as described in the legend to Fig. 1*B*, and whole cell lysates were prepared and assayed for aconitase and SDH activity as described under "Experimental Procedures." Units are represented as either nanomoles of *cis*-aconitate converted/mg of protein/min (aconitase), or nanomoles of 2,6-dichlorindophenol reduced/mg of protein/min (SDH); values represent the average of triplicate samples; *error bars* = S.D. The data are representative of 6–9 independent cultures analyzed over 2–3 experimental trials, with the possible exception of paraquat effects on *sod2*Δ aconitase. Paraquat either had little impact on the low aconitase of *sod2*Δ cells (as shown) or, in some studies, would increase this activity, perhaps reflecting the induction of the corresponding gene by severe oxidative stress (70). *B*, the indicated cells were spotted on glycerol containing medium as described in the legend to Fig. 1*A*, and after the indicated incubation times in days, cells were harvested and assayed for aconitase and SDH activity. The data are representative of 2–3 independent experimental trials, each run in duplicate; *error bars* = S.D. *C*, the indicated intracellular metabolites were measured by gas chromatography mass spectrometry as described under "Experimental Procedures." Values represent averages of duplicate samples; *error bars* = S.D.

paraquat, extracellular acetate levels rise dramatically to levels comparable with that seen with high glucose (Fig. 7, *A* and *B*). The high expulsion of acetate into the growth medium was also seen in *sod2*Δ cells treated with low paraquat (Fig. 7*B*) and with all the acid producing TCA cycle mutants (*sdh2*Δ, *cit1*Δ, *aco1*Δ, *kgd1*Δ, and *fum1*Δ) (Fig. 7*D*). In every case where cells make acid with low glucose, there is ≥100-fold higher levels of extracellular acetate in the growth medium than is seen with control cells not producing acid (Fig. 7, *A*, *B*, and *D*, and Table 2). Intracellular acetate is also elevated, albeit not to the same degree as extracellular acetate (Fig. 7, *C* and *E*). The high level of extracellular acetate can easily account for the acid burst observed, as spiking the growth medium with levels of acetic acid produced in paraquat-treated cells (0.276 μg/μl) was sufficient to lower the pH to roughly the same degree (Table 2).

The acetate that normally enters the TCA cycle can be derived from the cytosolic and/or mitochondrial pyruvate dehydrogenase bypass pathways or from the hydrolysis of acetyl-CoA. In the pyruvate dehydrogenase bypass pathways, pyruvate is converted to acetaldehyde, which in turn, is converted to acetate via the action of aldehyde dehydrogenase (ALD) enzymes (62). *S. cerevisiae* expresses 5 aldehyde dehydrogenase isoforms (63) and we tested if mutants in any of these would prevent the acid burst. Of these, deletion of the major mitochondrial isoform Ald4p most significantly inhibited paraquat-induced acidification of the growth medium with low glucose (Fig. 8*A*). Loss of Ald4p also attenuated the constitutive acidification of low glucose medium by *sdh4*Δ mutants (Fig. 8*B*). Consistent with these reversals of acidification, we observed corresponding decreases in acetate production when *ald4*Δ is disrupted in paraquat-treated cells and in *sdh4*Δ mutants grown with low glucose (Fig. 7*F*). The effect of *ald4*Δ mutations was also examined in cells grown under long-term glycerol conditions. As seen in Fig. 8*C*, *ald4*Δ mutations prevented the early acid burst of *sod2*Δ cells on glycerol. Moreover, loss of *ALD4* in the background of *SOD2*+ cells completely prevented the acid burst with long-term respiratory conditions, and the extracellular pH continued to rise over time with *ald4*Δ mutants (Fig. 2). Under all cases studied, the acid burst produced by cells under glucose starvation is dependent on mitochondrial pyruvate dehydrogenase bypass enzyme, Ald4p.

Conditioning the Growth Medium by the Acid Burst—What is the significance of the Acid Burst? As one possibility, cells

TABLE 1

Effects of TCA and ETC mutants on extracellular pH

pH was measured as described under "Experimental Procedures" after the indicated strains were grown 24 h in 0.2% glucose growth medium. The average pH of triplicate samples is denoted with S.D. in parentheses. For WT + PQ, WT cells were grown in media containing 800 μM paraquat (ETC, electron transport chain; mito, mitochondrial).

TCA mutants			ETC mutants		
Sample	**Description**	**pH**	**Sample**	**Description**	**pH**
No cells		5.53 (± 0.00)	No cells		5.43 (± 0.00)
WT		7.17 (± 0.05)	WT		6.90 (± 0.03)
WT + PQ		4.59 (± 0.03)	WT + PQ		4.67 (± 0.03)
*sdh2*Δ	Succinate dehydrogenase	4.54 (± 0.05)	*sdh2*Δ	Complex II	4.47 (± 0.02)
*sdh4*Δ		4.55 (± 0.04)	*sdh4*Δ		4.47 (± 0.02)
*cit1*Δ	Citrate synthase	4.54 (± 0.02)	*coq1*Δ	Coenzyme Q	5.19 (± 0.01)
*aco1*Δ	Aconitase	4.64 (± 0.02)	*cyt1*Δ	Complex III	5.21 (± 0.03)
*idh1*Δ	Isocitrate dehydrogenase	5.46 (± 0.10)	*cox7*Δ	Complex IV	5.20 (± 0.03)
*kgd1*Δ	α-ketoglutarate dehydrogenase	4.72 (± 0.01)	*rho*$^-$	No mito DNA	5.17 (± 0.03)
*lsc1*Δ	Succinyl-CoA ligase	6.42 (± 0.08)			
*fum1*Δ	Fumarase	4.71 (± 0.01)			
*mdh1*Δ	Malate dehydrogenase	7.14 (± 0.07)			

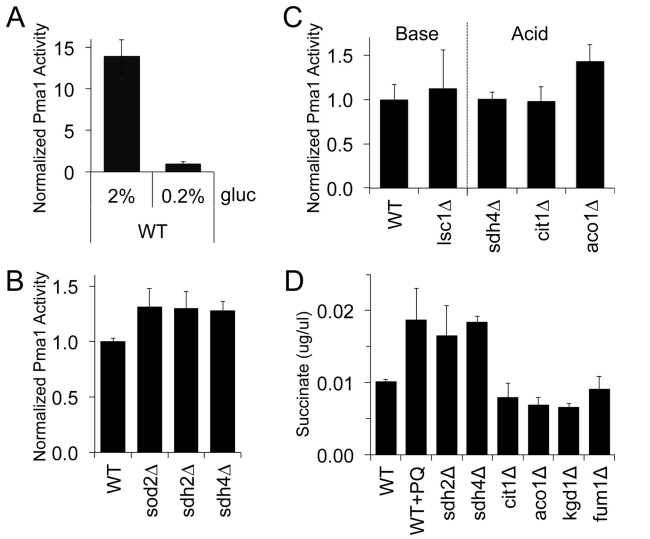

FIGURE 6. **Acid production with low glucose does not correlate with activation of Pma1p or with extracellular succinate.** *A–C*, the indicated yeast strains were grown in either 2 (*A*) or 0.2% (*A–C*) glucose to mid-log phase, and Pma1p activity was measured in membranes by orthovanadate-sensitive ATPase activity as described under "Experimental Procedures." Values are shown normalized to WT cells in 0.2% glucose, and represent the average of duplicate measurements; *error bars* = S.D. *C, base* and *acid* reflects the corresponding effect of the yeast strain on extracellular medium in 0.2% glucose. *D*, extracellular succinate levels were measured in the growth medium as described under "Experimental Procedures" from the indicated cells that had been cultured in 0.2% glucose for 24 h. *+PQ* = WT cells grown with 800 μM paraquat.

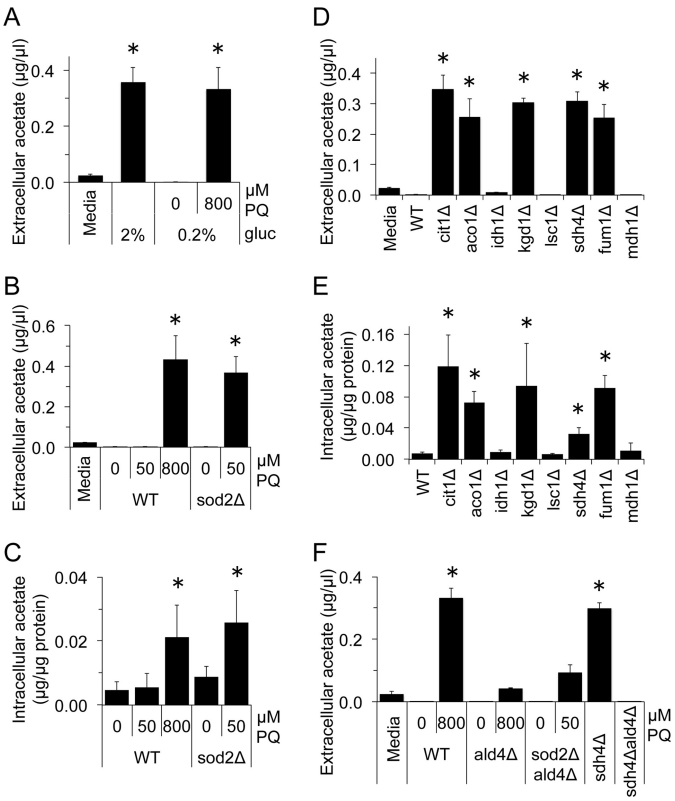

FIGURE 7. **Cells produce high levels of extracellular acetate during the acid burst.** *A*, *B*, *D*, and *F*, extracellular acetate was measured in the growth medium of WT cells (*A*) or the indicated strains grown in either 2 (*A*) or 0.2% (*A–F*) glucose for 24 h in the presence of the designated concentrations of paraquat (*PQ*). *Media* = levels of acetate in the starting growth medium with no cells. *C* and *E*, intracellular acetate was measured in the indicated cells according to "Experimental Procedures." Results represent the averages of triplicate samples; *error bars* = S.D. *Asterisks* denote the particular conditions and strains in which cells acidify the growth medium.

might produce copious amounts of acetate to provide a carbon source for neighboring cells under conditions of long-term carbon source starvation. To determine whether acetate production and/or media acidification could enhance growth of yeast cells, we collected "conditioned" growth media that was conditioned by cells grown 24 h in low glucose. Low acetate/high pH medium was obtained from cultures of WT and *ald4*Δ cells, and high acetate/low pH medium was obtained from cultures of *sdh4*Δ cells and from *sod2*Δ cells treated with 50 μM paraquat, a low dose that is non-toxic to WT cells (Fig. 4*C*). After removal of cells by filtration, these various conditioned media were used to inoculate WT cells and growth was monitored over 10 h. As seen in Fig. 9*A*, the high acetate/low pH media of *sdh4*Δ and paraquat-treated *sod2*Δ cells supported strong growth of WT cells, whereas the low acetate/high pH media from WT cells or from *ald4*Δ mutants was poorly effective at supporting growth. To determine whether acetate alone accounts for these differences, we supplemented the low acetate medium from WT and *ald4*Δ cells with levels of glacial acetic acid (0.20 – 0.22 μg/μl) equivalent to that in cultures of *sdh4*Δ and paraquat-treated *sod2*Δ cells. This supplementation of acetic acid was sufficient to eliminate differences in the various conditioned media, and all four media types supported growth of WT cells (Fig. 9*B*). Thus, the production of acetate can enhance growth of yeast cells under glucose starvation. This event triggered by superoxide disruptions in the TCA cycle may enable the organism to withstand long-term periods of starvation.

TABLE 2

Contribution of acetic acid to pH of growth medium

Acetic acid and pH levels were measured as described under "Experimental Procedures" in 0.1% glucose growth medium (starting pH 5.55) that was cultured where indicated (WT cells) for 24 h with WT yeast grown ± paraquat. Supplementation of medium with 0.25 μg/μl of acetic acid is sufficient to drop pH to levels seen in medium from paraquat-treated WT cells.

Sample	Acetate	pH
	$\mu g/\mu l$	
WT cells	Undetectable	6.46
WT cells + 800 μM PQ	0.276	4.87
No cells	0.026	5.55
No cells + 0.25 μg/μl glacial acetic acid	0.278	4.93

DISCUSSION

Herein, we describe a mechanism by which the *S. cerevisiae* yeast modifies its extracellular environment during prolonged nutrient depravation. Under long-term colonization on respiratory carbon sources, yeast cells shift from alkalization to producing acid and we demonstrate here that this acid burst is dependent on the acetate-producing Ald4p aldehyde dehydrogenase. Media conditioned by Ald4-acetate is indeed able to promote yeast cell growth under glucose starvation conditions. Our findings are consistent with a model in which the acid burst is produced in response to disruption of the TCA cycle by superoxide (Fig. 9*C*).

Perhaps the most intriguing finding of this work is the apparent role of mitochondrial matrix superoxide in conditioning the extracellular environment. Mitochondrial superoxide is not likely to cross mitochondrial membranes (30) and yet it can

influence extracellular pH by modulating organic acid production. In support of this effect of mitochondrial superoxide, we observed that the acid burst under long-term glycerol conditions is accelerated by *sod2*Δ mutations lacking mitochondrial matrix Mn-SOD, but not by *sod1*Δ mutations affecting the largely cytosolic Cu,Zn-SOD1. Previously, the loss of Sod2p was shown to reduce volatile ammonia production and prevent transition to the alkali phase under long-term glycerol conditions but the mechanism was unknown (19). This may be explained by the early acid burst of *sod2*Δ cells which by lowering pH would trap a significant portion of ammonia ($pK_a \approx$ 9.25) in the non-volatile ammonium form. Alternatively, Sod2p may have separable roles in regulating extracellular pH through ammonia and acetate production.

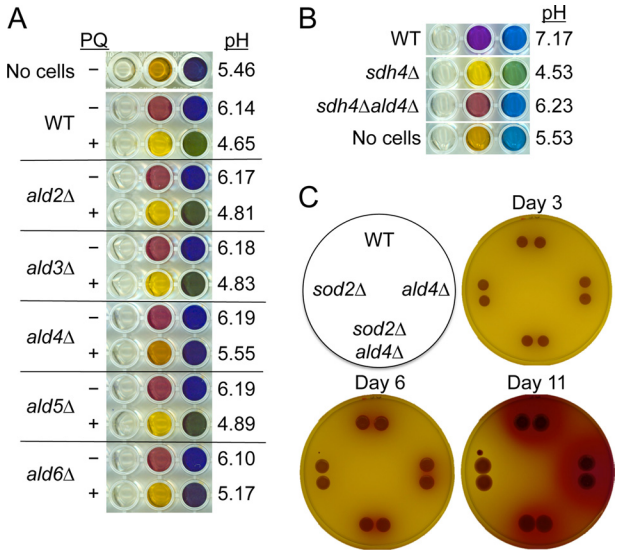

FIGURE 8. **The mitochondrial Ald4p aldehyde dehydrogenase is required for the acid burst.** The indicated strains were grown either in low glucose liquid medium (*A* and *B*) or on glycerol containing plates (*C*) and pH was monitored as described in the legend to Fig. 1. *A* and *B*, pH values represent the results of duplicate (*A*) or triplicate (*B*) samples where S.D. ≤0.12. +*PQ* = cultures supplemented with 800 μM paraquat.

In further support of the role of superoxide in triggering the acid burst, we observe that acid production under both glycerol and low glucose conditions is dramatically accelerated when WT cells are treated with the redox cycler paraquat; conversely, the acid burst with long-term glycerol conditions is eliminated by Mn-antioxidants, chemical mimics of SOD enzymes that can remove superoxide in yeast (44–50). Superoxide, more specifically mitochondrial superoxide, represents an ideal candidate to initiate the acid burst. Key Fe-S cluster enzymes in the TCA cycle (*i.e.* SDH and aconitase) are sensitive to superoxide inactivation (24–26, 54, 55), and we show here that disruption in the TCA cycle can cause build-up of acetate derived from mitochondrial Ald4p. Although multiple reports have established a role for ROS in cell signaling and regulation (64–67), the inactivation of TCA cycle enzymes by mitochondrial superoxide was up until now considered a detrimental outcome of oxidative damage. This is, perhaps, the first example where superoxide inactivation of mitochondrial enzymes can be beneficial, particularly under the stress conditions of nutrient depravation.

Superoxide is a natural by-product of respiration, yet in WT cells the acid burst only occurs after prolonged incubations under respiratory conditions (as in Fig. 2). The products of superoxide damage appear to accumulate slowly in these cells, as we observe a gradual loss in SDH activity over prolonged respiratory growth (Fig. 5*B*). In *sod2*Δ cells the combined effects of this slow loss in SDH together with the already low aconitase of these cells can explain the acceleration in the acid burst observed. Once SDH and/or aconitase activity have been sufficiently inhibited to disrupt TCA cycle functioning, the Ald4p acid burst occurs. In the simplest model, the blockage in

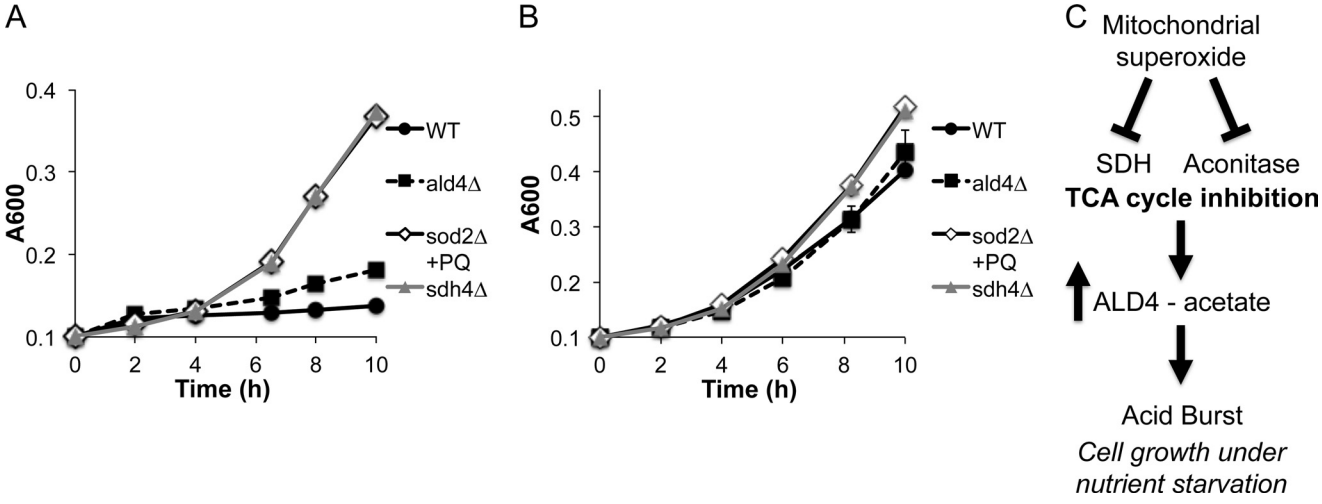

FIGURE 9. **Medium conditioned during the acid burst can promote yeast growth.** Growth medium was collected from the indicated cultures following 24 h incubation in 0.2% glucose medium. This cell-free "conditioned medium" was used to inoculate WT cultures of yeast as described under "Experimental Procedures" and growth was monitored turbidimetrically at A_{600}. Results represent the averages of triplicate cultures; *error bars* = S.D. In some cases, the error was too small to be seen by *error bars*. *A*, conditioned medium was used as isolated from cells. *B*, the levels of acetate in all four types of conditioned medium were normalized by supplementing 0.20–0.22 μg/μl of glacial acetic acid to the medium conditioned by WT and *ald4*Δ cells. *C*, a model for how mitochondrial superoxide produced during long-term respiratory conditions can lead to the acid burst and conditioning of the extracellular environment. Superoxide can lead to disruption of the TCA cycle through damage to the Fe-S enzymes aconitase and/or SDH. The blockage in the TCA cycle causes a build up in acetate derived from the mitochondrial Ald4p aldehyde dehydrogenase. The high levels of acetate expelled into the growth medium can condition the extracellular environment to promote growth under glucose starvation conditions.

the TCA cycle itself prevents mitochondrial consumption of Ald4-acetate, and the accumulated metabolite is expelled from the cell. Ald4 production of acetate might also be enhanced in a futile attempt to correct the TCA cycle defect. It is noteworthy that blockages in 5 of 8 steps in the TCA cycle resulted in an acetate burst, including losses in SDH and aconitase, as well as citrate dehydrogenase, α-ketoglutarate dehydrogenase, and fumarase. It is possible that mutants for the remaining three steps (*idh1*Δ, *mdh1*Δ, and *lsc1*Δ (68, 69)) do not yield the same disruption in TCA cycle functioning.

Although high acetate has previously been associated with increased chronological aging in yeast (8, 9), these previous studies were conducted with fermenting yeast cells with abundant glucose. In contrast, our studies with respiring yeast (as in Fig. 9) indicate that high acetate can be beneficial in environments with scarce nutrients. Overall, these studies provide the first line of evidence for mitochondrial superoxide and the TCA cycle in conditioning the extracellular environment under glucose starvation conditions.

Acknowledgments—We thank Dr. Amit Reddi for helpful discussions, Dr. Z. Palkova for suggestions on giant colony analyses, and C. Vazquez for technical support.

REFERENCES

1. Mbengue, A., Yam, X. Y., and Braun-Breton, C. (2012) Human erythrocyte remodelling during *Plasmodium falciparum* malaria parasite growth and egress. *Br. J. Haematol.* **157,** 171–179
2. Friedl, P., and Alexander, S. (2011) Cancer invasion and the microenvironment. Plasticity and reciprocity. *Cell* **147,** 992–1009
3. Martínez-Zaguilán, R., Seftor, E. A., Seftor, R. E., Chu, Y. W., Gillies, R. J., and Hendrix, M. J. (1996) Acidic pH enhances the invasive behavior of human melanoma cells. *Clin. Exp. Metastasis* **14,** 176–186
4. Hirschhaeuser, F., Sattler, U. G., and Mueller-Klieser, W. (2011) Lactate. A metabolic key player in cancer. *Cancer Res.* **71,** 6921–6925
5. Merkel, O., Fido, M., Mayr, J. A., Prüger, H., Raab, F., Zandonella, G., Kohlwein, S. D., and Paltauf, F. (1999) Characterization and function *in vivo* of two novel phospholipases B/lysophospholipases from *Saccharomyces cerevisiae*. *J. Biol. Chem.* **274,** 28121–28127
6. Jules, M., Guillou, V., François, J., and Parrou, J. (2004) Two distinct pathways for trehalose assimilation in the yeast *Saccharomyces cerevisiae*. *Appl. Environ. Microbiol.* **70,** 2771–2778
7. Vogel, K., and Hinnen, A. (1990) The yeast phosphatase system. *Mol. Microbiol.* **4,** 2013–2017
8. Burtner, C. R., Murakami, C. J., Kennedy, B. K., and Kaeberlein, M. (2009) A molecular mechanism of chronological aging in yeast. *Cell Cycle* **8,** 1256–1270
9. Burtner, C. R., Murakami, C. J., Olsen, B., Kennedy, B. K., and Kaeberlein, M. (2011) A genomic analysis of chronological longevity factors in budding yeast. *Cell Cycle* **10,** 1385–1396
10. Hayashi, M., Ohkuni, K., and Yamashita, I. (1998) Control of division arrest and entry into meiosis by extracellular alkalisation in *Saccharomyces cerevisiae*. *Yeast* **14,** 905–913
11. Portillo, F. (2000) Regulation of plasma membrane H^+-ATPase in fungi and plants. *Biochim. Biophys. Acta* **1469,** 31–42
12. Sigler, K., Kotyk, A., Knotková, A., and Opekarová, M. (1981) Processes involved in the creation of buffering capacity and in substrate-induced proton extrusion in the yeast *Saccharomyces cerevisiae*. *Biochim. Biophys. Acta* **643,** 583–592
13. Burhans, W. C., and Weinberger, M. (2009) Acetic acid effects on aging in budding yeast. Are they relevant to aging in higher eukaryotes? *Cell Cycle* **8,** 2300–2302
14. van der Rest, M. E., Kamminga, A. H., Nakano, A., Anraku, Y., Poolman, B., and Konings, W. N. (1995) The plasma membrane of *Saccharomyces cerevisiae*. Structure, function, and biogenesis. *Microbiol. Rev.* **59,** 304–322
15. Palková, Z., Janderová, B., Gabriel, J., Zikánová, B., Pospísek, M., and Forstová, J. (1997) Ammonia mediates communication between yeast colonies. *Nature* **390,** 532–536
16. Palková, Z., and Vachova, L. (2003) Ammonia signaling in yeast colony formation. *Int. Rev. Cytol.* **225,** 229–272
17. Palková, Z., and Forstová, J. (2000) Yeast colonies synchronise their growth and development. *J. Cell Sci.* **113,** 1923–1928
18. Palková, Z., Devaux, F., Icicová, M., Mináriková, L., Le Crom, S., and Jacq, C. (2002) Ammonia pulses and metabolic oscillations guide yeast colony development. *Mol. Biol. Cell* **13,** 3901–3914
19. Cáp, M., Váchová, L., and Palková, Z. (2009) Yeast colony survival depends on metabolic adaptation and cell differentiation rather than on stress defense. *J. Biol. Chem.* **284,** 32572–32581
20. Palková, Z., Váchová, L., Gásková, D., and Kucerová, H. (2009) Synchronous plasma membrane electrochemical potential oscillations during yeast colony development and aging. *Mol. Membr. Biol.* **26,** 228–235
21. Cáp, M., Váchová, L., and Palková, Z. (2010) How to survive within a yeast colony. Change metabolism or cope with stress?. *Commun. Integr. Biol.* **3,** 198–200
22. Sturtz, L. A., Diekert, K., Jensen, L. T., Lill, R., and Culotta, V. C. (2001) A fraction of yeast Cu,Zn-superoxide dismutase and its metallochaperone, CCS, localize to the intermembrane space of mitochondria. *J. Biol. Chem.* **276,** 38084–38089
23. Weisiger, R. A., and Fridovich, I. (1973) Mitochondrial superoxide dismutase. *J. Biol. Chem.* **248,** 4793–4796
24. Melov, S., Coskun, P., Patel, M., Tuinstra, R., Cottrell, B., Jun, A. S., Zastawny, T. H., Dizdaroglu, M., Goodman, S. I., Huang, T. T., Miziorko, H., Epstein, C. J., and Wallace, D. C. (1999) Mitochondrial disease in superoxide dismutase 2 mutant mice. *Proc. Natl. Acad. Sci. U.S.A.* **96,** 846–851
25. Li, Y., Huang, T. T., Carlson, E. J., Melov, S., Ursell, P. C., Olson, J. L., Noble, L. J., Yoshimura, M. P., Berger, C., Chan, P. H., Wallace, D. C., and Epstein, C. J. (1995) Dilated cardiomyopathy and neonatal lethality in mutant mice lacking manganese superoxide dismutase. *Nat. Genet.* **11,** 376–381
26. Kirby, K., Hu, J., Hilliker, A. J., and Phillips, J. P. (2002) RNA interference-mediated silencing of Sod2 in *Drosophila* leads to early adult-onset mortality and elevated endogenous oxidative stress. *Proc. Natl. Acad. Sci. U.S.A.* **99,** 16162–16167
27. Outten, C. E., Falk, R. L., and Culotta, V. C. (2005) Cellular factors required for protection from hyperoxia toxicity in *Saccharomyces cerevisiae*. *Biochem. J.* **388,** 93–101
28. Guidot, D. M., McCord, J. M., Wright, R. M., and Repine, J. E. (1993) Absence of electron transport (Rho 0 state) restores growth of a manganese-superoxide dismutase-deficient *Saccharomyces cerevisiae* in hyperoxia. Evidence for electron transport as a major source of superoxide generation *in vivo*. *J. Biol. Chem.* **268,** 26699–26703
29. Demir, A. B., and Koc, A. (2010) Assessment of chronological lifespan dependent molecular damages in yeast lacking mitochondrial antioxidant genes. *Biochem. Biophys. Res. Commun.* **400,** 106–110
30. Gus'kova, R. A., Ivanov, I. I., Kol'tover, V. K., Akhobadze, V. V., and Rubin, A. B. (1984) Permeability of bilayer lipid membranes for superoxide (O_2^-) radicals. *Biochim. Biophys. Acta* **778,** 579–585
31. Outten, C. E., and Culotta, V. C. (2003) A novel NADH kinase is the mitochondrial source of NADPH in *Saccharomyces cerevisiae*. *EMBO J.* **22,** 2015–2024
32. Luk, E., Carroll, M., Baker, M., and Culotta, V. C. (2003) Manganese activation of superoxide dismutase 2 in *Saccharomyces cerevisiae* requires MTM1, a member of the mitochondrial carrier family. *Proc. Natl. Acad. Sci. U.S.A.* **100,** 10353–10357
33. Culotta, V. C., Klomp, L. W., Strain, J., Casareno, R. L., Krems, B., and Gitlin, J. D. (1997) The copper chaperone for superoxide dismutase. *J. Biol. Chem.* **272,** 23469–23472
34. Sikorski, R. S., and Hieter, P. (1989) A system of shuttle vectors and yeast host strains designed for efficient manipulation of DNA in *Saccharomyces*

cerevisiae. *Genetics* **122,** 19–27
35. Schiestl, R. H., and Gietz, R. D. (1989) High efficiency transformation of intact yeast cells using single stranded nucleic acids as a carrier. *Curr. Genet.* **16,** 339–346
36. Gleason, J. E., Corrigan, D. J., Cox, J. E., Reddi, A. R., McGinnis, L. A., and Culotta, V. C. (2011) Analysis of hypoxia and hypoxia-like states through metabolite profiling. *PLoS One* **6,** e24741
37. Ackrell, B. A., Kearney, E. B., and Singer, T. P. (1978) Mammalian succinate dehydrogenase. *Methods Enzymol.* **53,** 466–483
38. Perlin, D. S., Harris, S. L., Seto-Young, D., and Haber, J. E. (1989) Defective H^+-ATPase of hygromycin B-resistant pma1 mutants from *Saccharomyces cerevisiae*. *J. Biol. Chem.* **264,** 21857–21864
39. Monk, B. C., Kurtz, M. B., Marrinan, J. A., and Perlin, D. S. (1991) Cloning and characterization of the plasma membrane H^+-ATPase from *Candida albicans*. *J. Bacteriol.* **173,** 6826–6836
40. Pedrajas, J. R., Kosmidou, E., Miranda-Vizuete, A., Gustafsson, J. A., Wright, A. P., and Spyrou, G. (1999) Identification and functional characterization of a novel mitochondrial thioredoxin system in *Saccharomyces cerevisiae*. *J. Biol. Chem.* **274,** 6366–6373
41. Lee, J., Spector, D., Godon, C., Labarre, J., and Toledano, M. B. (1999) A new antioxidant with alkyl hydroperoxide defense properties in yeast. *J. Biol. Chem.* **274,** 4537–4544
42. Chae, H. Z., Chung, S. J., and Rhee, S.G. (1994) Thioredoxin-dependent peroxide reductase from yeast. *J. Biol. Chem.* **269,** 27670–27678
43. Inoue, Y., Matsuda, T., Sugiyama, K., Izawa, S., and Kimura, A. (1999) Genetic analysis of glutathione peroxidase in oxidative stress response of *Saccharomyces cerevisiae*. *J. Biol. Chem.* **274,** 27002–27009
44. Aguirre, J. D., and Culotta, V. C. (2012) Battles with iron. Manganese in oxidative stress protection. *J. Biol. Chem.* **287,** 13541–13548
45. Reddi, A. R., and Culotta, V. C. (2011) Regulation of manganese antioxidants by nutrient sensing pathways in *Saccharomyces cerevisiae*. *Genetics* **189,** 1261–1270
46. Reddi, A. R., Jensen, L. T., Naranuntarat, A., Rosenfeld, L., Leung, E., Shah, R., and Culotta, V. C. (2009) The overlapping roles of manganese and Cu/Zn-SOD in oxidative stress protection. *Free Radic. Biol. Med.* **46,** 154–162
47. Sanchez, R. J., Srinivasan, C., Munroe, W. H., Wallace, M. A., Martins, J., Kao, T. Y., Le, K., Gralla, E. B., and Valentine, J. S. (2005) Exogenous manganous ion at millimolar levels rescues all known dioxygen-sensitive phenotypes of yeast lacking CuZnSOD. *J. Biol. Inorg. Chem.* **10,** 913–923
48. Lapinskas, P. J., Cunningham, K. W., Liu, X. F., Fink, G. R., and Culotta, V. C. (1995) Mutations in PMR1 suppress oxidative damage in yeast cells lacking superoxide dismutase. *Mol. Cell. Biol.* **15,** 1382–1388
49. Barnese, K., Gralla, E. B., Cabelli, D. E., and Valentine, J. S. (2008) Manganous phosphate acts as a superoxide dismutase. *J. Am. Chem. Soc.* **130,** 4604–4606
50. Barnese, K., Gralla, E. B., Valentine, J. S., and Cabelli, D. E. (2012) Biologically relevant mechanism for catalytic superoxide removal by simple manganese compounds. *Proc. Natl. Acad. Sci. U.S.A.* **109,** 6892–6897
51. Cochemé, H. M., and Murphy, M. P. (2008) Complex I is the major site of mitochondrial superoxide production by paraquat. *J. Biol. Chem.* **283,** 1786–1798
52. Cochemé, H. M., and Murphy, M. P. (2009) The uptake and interactions of the redox cycler paraquat with mitochondria. *Methods Enzymol.* **456,** 395–417
53. Blaszczyński, M., Litwińska, J., Zaborowska, D., and Biliński, T. (1985) The role of respiratory chain in paraquat toxicity in yeast. *Acta Microbiol. Pol.* **34,** 243–254
54. Keyer, K., and Imlay, J. (1996) Superoxide accelerates DNA damage by elevating free-iron levels. *Proc. Natl. Acad. Sci. U.S.A.* **93,** 13635–13640
55. Wallace, M. A., Liou, L. L., Martins, J., Clement, M. H., Bailey, S., Longo, V. D., Valentine, J. S., and Gralla, E. B. (2004) Superoxide inhibits 4Fe-4S cluster enzymes involved in amino acid biosynthesis. *J. Biol. Chem.* **279,** 32055–32062
56. Strain, J., Lorenz, C. R., Bode, J., Garland, S., Smolen, G.A., Ta, D. T., Vickery, L. E., and Culotta, V. C. (1998) Suppressors of superoxide dismutase (SOD1) deficiency in *Saccharomyces cerevisiae*. Identification of proteins predicted to mediate iron-sulfur cluster assembly. *J. Biol. Chem.* **273,** 31138–31144
57. Navarro-Sastre, A., Tort, F., Stehling, O., Uzarska, M. A., Arranz, J. A., Del Toro, M., Labayru, M. T., Landa, J., Font, A., Garcia-Villoria, J., Merinero, B., Ugarte, M., Gutierrez-Solana, L. G., Campistol, J., Garcia-Cazorla, A., Vaquerizo, J., Riudor, E., Briones, P., Elpeleg, O., Ribes, A., and Lill, R. (2011) A fatal mitochondrial disease is associated with defective NFU1 function in the maturation of a subset of mitochondrial Fe-S proteins. *Am. J. Hum. Genet.* **89,** 656–667
58. Sheftel, A. D., Stehling, O., Pierik, A. J., Netz, D. J., Kerscher, S., Elsässer, H. P., Wittig, I., Balk, J., Brandt, U., and Lill, R. (2009) Human Ind1, an iron-sulfur cluster assembly factor for respiratory complex I. *Mol. Cell. Biol.* **29,** 6059–6073
59. Sheftel, A. D., Wilbrecht, C., Stehling, O., Niggemeyer, B., Elsässer, H. P., Mühlenhoff, U., and Lill, R. (2012) The human mitochondrial ISCA1, ISCA2, and IBA57 proteins are required for [4Fe-4S] protein maturation. *Mol. Biol. Cell* **23,** 1157–1166
60. Szeto, S. S., Reinke, S. N., Sykes, B. D., and Lemire, B. D. (2007) Ubiquinone-binding site mutations in the *Saccharomyces cerevisiae* succinate dehydrogenase generate superoxide and lead to the accumulation of succinate. *J. Biol. Chem.* **282,** 27518–27526
61. Szeto, S. S., Reinke, S. N., Sykes, B. D., and Lemire, B. D. (2010) Mutations in the *Saccharomyces cerevisiae* succinate dehydrogenase result in distinct metabolic phenotypes revealed through ^{1}H NMR-based metabolic footprinting. *J. Proteome Res.* **9,** 6729–6739
62. Boubekeur, S., Bunoust, O., Camougrand, N., Castroviejo, M., Rigoulet, M., and Guérin, B. (1999) A mitochondrial pyruvate dehydrogenase bypass in the yeast *Saccharomyces cerevisiae*. *J. Biol. Chem.* **274,** 21044–21048
63. Navarro-Aviño, J. P., Prasad, R., Miralles, V. J., Benito, R. M., and Serrano, R. (1999) A proposal for nomenclature of aldehyde dehydrogenases in *Saccharomyces cerevisiae* and characterization of the stress-inducible *ALD2* and *ALD3* genes. *Yeast* **15,** 829–842
64. Mittler, R., Vanderauwera, S., Suzuki, N., Miller, G., Tognetti, V. B., Vandepoele, K., Gollery, M., Shulaev, V., and Van Breusegem, F. (2011) ROS signaling. The new wave?. *Trends Plant Sci.* **16,** 300–309
65. Meng, T. C., Fukada, T., and Tonks, N. K. (2002) Reversible oxidation and inactivation of protein tyrosine phosphatases *in vivo*. *Mol. Cell.* **9,** 387–399
66. Prosser, B. L., Ward, C. W., and Lederer, W. J. (2011) X-ROS signaling. Rapid mechanochemo transduction in heart. *Science* **333,** 1440–1445
67. D'Autréaux, B., and Toledano, M. B. (2007) ROS as signalling molecules. Mechanisms that generate specificity in ROS homeostasis. *Nat. Rev. Mol. Cell Biol.* **8,** 813–824
68. McCammon, M. T. (1996) Mutants of *Saccharomyces cerevisiae* with defects in acetate metabolism. Isolation and characterization of Acn^- mutants. *Genetics* **144,** 57–69
69. Sumegi, B., McCammon, M. T., Sherry, A. D., Keys, D. A., McAlister-Henn, L., and Srere, P. A. (1992) Metabolism of [3-^{13}C]pyruvate in TCA cycle mutants of yeast. *Biochemistry* **31,** 8720–8725
70. Gasch, A. P., Spellman, P. T., Kao, C. M., Carmel-Harel, O., Eisen, M. B., Storz, G., Botstein, D., and Brown, P. O. (2000) Genomic expression programs in the response of yeast cells to environmental changes. *Mol. Biol. Cell* **11,** 4241–4257